Biosensors and Bioelectronics 183 (2021) 113233

Contents lists available at ScienceDirect

Biosensors and Bioelectronics

journal homepage: http://www.elsevier.com/locate/bios

"Aptamer-locker" DNA coupling with CRISPR/Cas12a-guided biosensing for high-efficiency melamine analysis

Bin Qiao [a,****], Jiakun Xu [b,***], Wenhao Yin [c,d], Wanmeng Xin [c,d], Lixin Ma [c,d], Jie Qiao [c,d,**], Yi Liu [c,d,*]

[a] Department of Oral and Maxillofacial Surgery, The First Affiliated Hospital of Zhengzhou University, China
[b] Key Lab of Sustainable Development of Polar Fisheries, Ministry of Agriculture and Rural Affairs, Yellow Sea Fisheries Research Institute, Chinese Academy of Fishery Sciences, Lab for Marine Drugs and Byproducts of Pilot National Lab for Marine Science and Technology, China
[c] State Key Laboratory of Biocatalysts and Enzyme Engineering, Hubei University, China
[d] Hubei Key Laboratory of Industrial Biotechnology, School of Life Sciences, Hubei University, China

ARTICLE INFO

Keywords:
Aptamer
CRISPR/Cas12a
Melamine
Biosensor
On-site test

ABSTRACT

Herein, we report a method that combined "aptamer-locker" DNA with CRISPR/Cas12a-based biosensing for sensitive and rapid melamine analysis. Three strategies were harnessed for designing the DNA sensors that were well characterized by circular dichroism (CD) spectroscopy and isothermal titration calorimetry (ITC) in the absence and presence of melamine. The detection parameters were optimized to achieve good analytic performance. As a result, a limit of detection (LOD) as low as 38 nM was achieved, which is below the threshold (1.0 mg/kg) of allowable melamine in infant milk products. In addition, the sensors show high selectivity for melamine against other analogues such as cyanuric acid, ammeline and ammelide. Moreover, our method was effective for rapid melamine analysis in whole milk samples, with or without sample pretreatment, in less than 20 min. Adopting a commercially available portable fluorimeter, on-site analysis of melamine in milk was accomplished. The strategies demonstrated here can expand to detect other non-nucleic-acid targets by simply replacing the aptamers.

1. Introduction

Melamine has been commonly but illegally added to food and milk products to increase the apparent protein content. High-dosage melamine can result in serious kidney damage to pets and human beings (Duan et al., 2015; Nascimento et al., 2017). In the past decades, the food-safety problems caused by melamine contamination have led to thousands of renal failure cases, severe infant illness and even deaths (Guan et al., 2009). For instance, nearly 300000 children in China were reported to be intoxicated in 2008 due to over-dosage melamine in milk. A consequence of such incidents has been the limitation of melamine in infant milk products to concentrations below 1.0 mg/kg by the U.S. Federal Food and Drug Administration (FDA), the European Commission, and the Chinese government.

Various methods of detecting melamine have been established to date, such as mass spectroscopy (Chen et al., 2015; Domingo Edo et al., 2015), high-performance liquid chromatograph (HPLC) (Ehling et al., 2007; Wang et al., 2016), electrochemistry (Fu et al., 2016) and enzyme-linked immunosorbent assay (ELISA) (Choi et al., 2016; Lei et al., 2010). Nevertheless, many of these are time-consuming and require the use of expensive equipment, which limit their application in on-site test. In recent years, several simple and cost-effective methods have been addressed such limitations, e.g. nanoparticle (Hu et al., 2018; Jigyasa and Rajput 2018; Alipour et al., 2020) and aptamer (Gu et al. 2015, 2016; Xie et al., 2019) based sensors. However, many issues are still needed to be resolved, such as poor reproducibility, involvement of multiple reaction steps, and so on.

In the last few years, discovery and development of CRISPR (clustered regularly interspaced short palindromic repeats) associated proteins have revolutionized not only genome editing but also other areas,

* Corresponding author. State Key Laboratory of Biocatalysts and Enzyme Engineering, Hubei University, China.
** Corresponding author. State Key Laboratory of Biocatalysts and Enzyme Engineering, Hubei University, China.
*** Corresponding author.
**** Corresponding author.
E-mail addresses: qiaobin@zzu.edu.cn (B. Qiao), xujk@ysfri.ac.cn (J. Xu), jieqiao@hubu.edu.cn (J. Qiao), yiliu0825@hubu.edu.cn (Y. Liu).

https://doi.org/10.1016/j.bios.2021.113233
Received 28 February 2021; Received in revised form 1 April 2021; Accepted 5 April 2021
Available online 7 April 2021

including molecular diagnostics, such as nucleic acid sensors based on SHERLOCK (Gootenberg et al. 2017, 2018) and DETECTR (Chen et al., 2018). As a member of CRISPR-Cas enzymes, Cas12a (Cpf1) shows a unique collateral DNase activity which can indiscriminately cleave any single strand DNA (ssDNA) substrates near the target double strand DNA (dsDNA) or crRNA-complementary ssDNA. Taking advantage of such property, various nucleic-acid-related diagnostics have been developed (Broughton et al., 2020; Myhrvold et al., 2018; Wang et al., 2021). More recently, Cas12a-based analytical methods have been expanded to detect non-nucleic-acid targets, e.g. transcription factors (Li et al., 2020a), biological enzymes (Du et al., 2021; Wang et al., 2020), and small molecules (Broughton et al., 2020; Li et al., 2020b; Xiong et al., 2020). Integrated with a portable fluorimeter (Xiong et al., 2020) or a mobile phone microscopy (Fozouni et al., 2020), these methods have the great potential for on-site test.

To develop a high-efficiency method for melamine analysis, we herein harnessed three strategies to construct the "aptamer-locker" CRISPR/Cas12a sensors. Circular dichroism (CD) spectroscopy and isothermal titration calorimetry (ITC) measurements were performed to characterize these DNA sensors. Consequently, one strategy failed while the other two succeed, producing sensor A and sensor C that could undergo structure changes upon addition of melamine. The quantitative analysis of melamine in solution was then conducted with use of sensor A and sensor C, achieving a LOD of 38 nM and 0.24 μM, respectively. For the practical use, we have investigated the quantification of melamine in milk. Good recovery was obtained according to a conventional protocol (Gu et al., 2016; Jigyasa and Rajput 2018) for pretreating the milk samples. More importantly, our method was effective for the detection of melamine in milk without any pretreatment (Hu et al., 2018), largely reducing the assay time. A standard test can be completed within 20 min under ambient temperatures. At last, the on-site detection of melamine in milk was accomplished by using a portable fluorimeter.

Together, we develop a method that combined "aptamer-locker" DNA with Cas12a-guided biosensing for high-efficiency melamine analysis. The method demonstrated here can be utilized to design biosensors for non-nucleic-acid targets.

2. Experimental

2.1. Materials and reagents

All DNA (including aptamer and locker DNA), crRNA and FAM-labeled ssDNA fluorescence reporters were ordered from Sangon Biotech (Shanghai). The sequences of the above oligonucleotides were listed in the supporting information. Melamine, RNase inhibitors were purchased from Beijing Solarbio Science & Technology Co., Ltd. Cyanuric acid, ammeline and ammelide were from Aladdin (Shanghai). The common chemicals for buffer preparation were from Sinopharm (Beijing). Mengniu and Guangming whole milk samples were purchased from local markets. A NANO ITC instrument (TA, USA) was utilized for isothermal titration calorimetry (ITC) assays. A Chrisman V100 circular dichroism spectrometer (Applied Photophysics, UK) was employed for the circular dichroism (CD) studies. A fluorescence spectrophotometer F4600 (Hitachi, Japan) was used for the fluorescence measurements. A portable fluorimeter (ANDalyze 1000 from ANDalyze, Inc., Champaign, USA) was used for recording the fluorescence signal at 520 nm following the manufacturer's protocol.

2.2. Circular dichroism (CD) spectroscopy

In the presence of melamine ranging from 0 to 100 μM, the CD spectra of aptamers, locker DNA and "aptamer-locker" sensors were recorded. A quartz cuvette (1 mm path length) was used for measuring the wavelengths ranging from 200 nm to 350 nm at 1 nm bandwidth, 1 nm step size, as well as 0.5 s per points. Buffer blank corrections were made for all the spectra.

2.3. Isothermal titration calorimetry (ITC)

The ITC experiments were carried out to determine the binding affinity between melamine and DNA aptamers in the absence and presence of locker DNA. All experiments were corrected for the heat of dilution. The melamine and target DNA samples were dissolved in buffer A (20 mM HEPES, 50 mM NaCl, 20 mM $MgCl_2$, pH 7.4). The vacuum degassing was performed before loading the samples into the cell and syringe. In a typical assay, 200 μM melamine was used to titrate 20 μM DNA samples in the cell. The ITC data can be fit by using different models, whereas one of the best-fitting results was chosen. According to the previous work (Gu et al., 2016), we employed the 1:1 binding model to fit the melamine titration data in this work. The fitting data represent the apparent melamine binding sites.

2.4. LbCas12a protein purification

Firstly, the protein expression vector having *Lachnospiraceae bacterium* ND2006 LbCas12a protein (LbCas12a, GI number: 917059416) gene cloned were transformed into *Escherichia coli* BL21 (DE3) competent cells. Following the protocol (Qiao et al. 2019, 2020) established in our lab, we purified the Cas12a proteins by running a Ni-NTA column and a secondary size exclusion column (HiLoad 16/60 Superdex 200). Using Millipore concentrators (100 KD), the purified LbCas12a proteins were concentrated in buffer B (pH 7.4, 50 mM Tris, 100 mM NaCl) and then analyzed by 10% SDS-PAGE (Fig. S1). The protein concentration was measured by Broadford method. At last, the concentrated Cas12a proteins were frozen at −80 °C.

2.5. Quantitative detection of melamine in solution

To achieve high-efficiency melamine analysis, three strategies were harnessed for designing the "aptamer-locker" DNA sensors (Fig. 1). For all melamine analysis experiments, the buffer A was used unless otherwise stated. The molar ratios of aptamer to locker DNA were firstly optimized to ensure a low background ratio of fluorescence signals. Among them, the sensor A was constructed by mixing the locker1 DNA and apatmer1 at a ratio of 1:1.5. Similarly, the sensor B was prepared by mixing the locker2 DNA and aptamer1 at a ratio of 1:1.5. Alternatively, the sensor C was prepared by mixing the locker3 DNA, aptamer2 and aptamer3 at a ratio of 1:1.5:1.5. To obtain stable "aptamer-locker" DNA complexes, the aptamer and locker DNA at a certain ratio were heated to 95 °C for 10 min followed by slow cooling down to 25 °C at a ratio of 0.1 °C per second. The final concentration of locker DNA and aptamer was 30 nM and 45 nM, respectively. The reporter solution (60 μL) containing Cas12a and ssDNA-FQ reporter DNA (FAM-TTATT-BHQ1) was prepared by mixing 20 μL of Cas12a protein (50 nM in buffer A) with 20 μL of crRNA (50 nM in RNase-free buffer) at 25 °C for 30 min, following by adding 20 μL of ssDNA-FQ (100 nM in buffer A).

To sensitively detect melamine, 20 μL of DNA sensors were added into 20 μL of buffer A containing different concentrations of melamine (0.1–100 μM). After that, 60 μL of reporter solution prepared above was added and incubated for 20 min at 25 °C. Next, the enzymatic reaction was stopped by heating at 70 °C for 5 min, and the fluorescence signal of the solution was measured by a fluorescence spectrophotometer F4600 (Hitachi, Japan). The excitation wavelength was 485 nm and emission wavelengths were monitored from 500 to 700 nm. To confirm the mechanism of sensors, we carried out PAGE analysis to detect the final products after enzymatic cleavage of the ssDNA substrates. The fluorescence data at 520 nm were plotted and analyzed using Origin 8.0 software.

2.6. Detection of melamine in milk samples

Firstly, the whole milk was pretreated according to the conventional protocols (Gu et al., 2016; Jigyasa and Rajput 2018). In a typical assay,

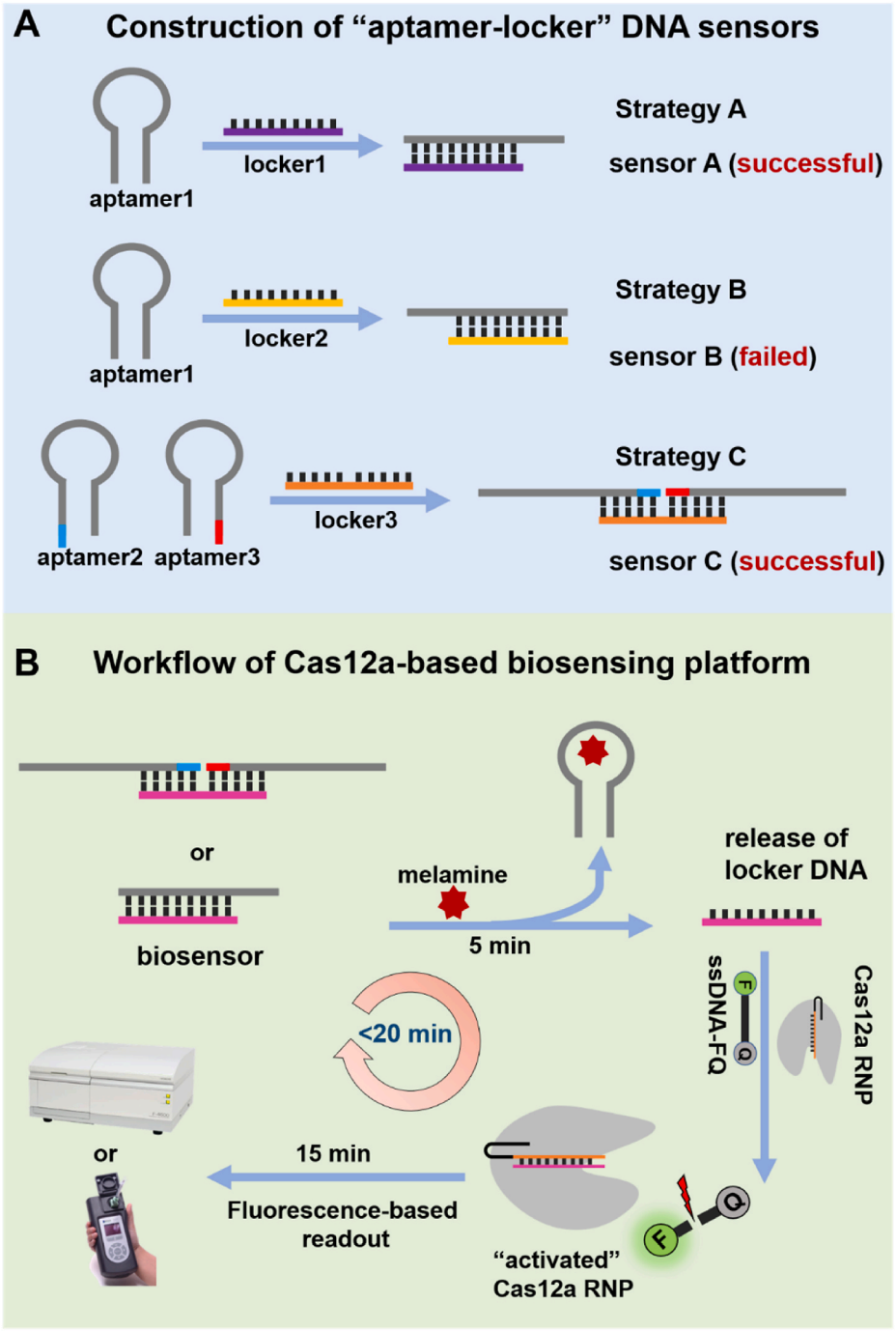

Fig. 1. Schematic of (A) three strategies for the construction of "aptamer-locker" DNA sensors, resulting in two successful sensors (sensor A and sensor C) and one failed sensor (sensor B); (B) the workflow of Cas12-based biosensing platform for sensitive and rapid melamine analysis.

about 3 mL of raw milk sample was mixed with 8 mL 10% trichloroacetic acid and 2 mL acetonitrile. The reaction mixtures were vortexed for 5 min and then centrifuged at 12000 rpm for 10 min to separate the protein precipitates. 1 M NaOH was added to the supernatant to adjust the pH to 7.0. The recovery efficiencies were validated in liquid milk samples by spiking different concentrations of melamine (Xie et al., 2019).

Next, we verified the possibility to detect the melamine in milk without any pretreatment. To obtain better fluorescence signals, the milk samples were diluted at different times. For example, we diluted the raw milk ten times with buffer A before each assay. Blank corrections were made for all the spectra by subtracting the fluorescence value of the diluted melamine-free milk.

For on-site assay, the fluorescence intensity of 520 nm was recorded by a portable fluorimeter (ANDalyze 1000 from ANDalyze, Inc., Champaign, USA).

3. Results and discussion

3.1. Design of "aptamer-locker" DNA sensors

Previously, Gu et al., (2016) reported a 34 nt stem-loop-structured aptamer termed Rd29C33-T7 (Fig. S2) that had high binding affinity and selectivity to melamine. Herein, we harnessed this

well-characterized DNA aptamer as the basic skeleton for designing melamine biosensors. The overall schematic of the method is shown in Fig. 1. Initially, the locker DNA binds to its corresponding melamine aptamer(s), resulting in the formation of three "aptamer-locker" DNA sensors. Upon addition of melamine, target binding to the aptamer would cause structure changes of the "aptamer-locker" sensors, leading to the release of locker DNA. After that, the releasing locker DNA binds to and activates the Cas12a ribonucleoprotein (RNP) consisting of a Cas12a protein and a crRNA. In this case, the "activated" Cas12a RNP indiscriminately cleaves the nearby ssDNA-FQ reporters, producing a significant increase of fluorescence signal at 520 nm. At last, the quantitative detection of melamine can be achieved by monitoring the fluorescence intensity changes using a fluorescence-based readout device.

3.2. Characterization of "aptamer-locker" DNA complexes

As shown in Fig. 1a, we harnessed three strategies for designing the "aptamer-locker" DNA sensors. To construct sensor A and sensor B, either a locker1 or a locker2 DNA was used to hybridize with a melamine aptamer1 at the 3′-end or 5′-end. To construct sensor C, a locker3 DNA was employed to simultaneously anchor two aptamers that were extended from the aptamer1 at its 5′ end with GTGTTT (aptamer2), or at its 3′ end with TTGTGTGT (aptamer3). The molar ratios of aptamer to locker DNA were firstly optimized by measuring the fluorescence signals (Fig. S3; the detailed discussion was shown in the supporting information). As a result, the ratio of aptamer to locker DNA at 1.5: 1 was chosen.

The CD spectra (Fig. 2) showed that all the aptamers had a positive peak at around 265 nm and a negative peak at around 240 nm, representing a parallel G-quadruplex (Yu et al., 2006). In contrast, the "aptamer-locker" DNA sensors showed red shift and the increase of original positive peak, along with the generation of another elevated peak at around 220 nm. These results indicate that all the DNA sensors were well assembled. In addition, we measured the spectra of them in the presence of melamine at different concentrations (Fig. S4). As a result, the addition of melamine to aptamer1 caused blue shift and the increase of 270 nm peak (Fig. S4A), which is consistent with the previous report (Gu et al., 2016). Similar results were obtained for sensor A (Fig. S4B) and sensor C (Fig. S 4D) but not for sensor B (Fig. S4C), indicating that these DNA sensors have distinct structure-switching abilities upon addition of melamine. In other words, the locker DNA could dehybridize from the "aptamer-locker" DNA complexes at different levels when melamine binds to the aptamer.

To measure the binding affinity of melamine to the aptamers and "aptamer-locker" sensors, isothermal titration calorimetry (ITC) experiments were performed. As shown in Fig. 3, the data were fit to a 1:1 binding model to obtain the dissociation constants (*K*d) and apparent target binding sites (Table S1). On one hand, the aptamer1 and sensor A showed similar binding sites (0.79 *vs* 0.59) and *K*d values (0.303 μM *vs* 0.338 μM), demonstrating that almost all of the sensor A could undergo structure switching upon addition of melamine. The sensor B showed a same-level affinity (*K*d = 0.258 μM) but had only 0.12 melamine binding site, indicating that the locker2 DNA could not efficiently dehybridize from the "aptamer1-locker2" complex even at a high concentration of melamine, for example, 25 μM in the final titration cell in this case. This result is consistent with the findings of CD (Fig. S4C). On the other hand, the sensor C had a comparable value (0.69) of melamine binding site to aptamer1. Nevertheless, it showed a much lower melamine binding affinity (K_d = 1.559 μM), suggesting it had undergone relatively weak structure changes in the presence of melamine. Taken together, sensor A and sensor C have proven to show the basis for developing Cas12a-guided fluorescent method.

3.3. Quantitative analysis of melamine

The fluorescent studies were performed by adopting a 5 nt ssDNA-FQ. Once Cas12a RNP was activated by recognizing the free locker DNA in solution, it cleaved the nearby ssDNA-FQ indiscriminately and generated a strong fluorescent signal at 520 nm (Fig. 4). In contrast, the Cas12a RNP with or without aptamers showed minimal fluorescence signals in the absence of locker DNA. Importantly, all the "aptamer-locker" DNA sensors showed inconsiderable fluorescence signals when incubated with Cas12a RNP and ssDNA-FQ, indicating that the locker DNA can efficiently prevent the activation of Cas12a RNP. When adding 200 μM melamine, both of sensor A (Fig. 4A) and sensor C (Fig. 4C) showed significant increases of fluorescence intensity at 520 nm, indicating the recovery of Cas12a collateral activity due to the release of locker DNA from "aptamer-locker" complexes. At the same time, very slight increases in fluorescence intensity were observed for sensor B (Fig. 4B). This reveals that the design of sensor B is failed, possibly due to the melamine binding sites were tightly blocked in this variant. Furthermore, the PAGE analysis experiments (Fig. 4D) confirmed that the designs of sensor A and sensor C were effective.

To quantitatively detect melamine, we measured the fluorescence spectra of sensor A and sensor C in the presence of melamine at different concentrations. The fluorescence signal at 520 nm was plotted, and the linear relationship was shown in the insets (Fig. 5). For sensor A, the fluorescence intensity at 520 nm elevated with the increasing of melamine concentration from 0.1 to 25 μM. The linear relationship is from 0 to 2.5 μM ($y = 1.157 + 25.780*C_{melamine}$, $R^2 = 0.976$). Fig. 5B shows the 520 nm signal of sensor C increased linearly with melamine concentrations ranging from 0 to 25 μM ($y = 2.103 + 4.111*C_{melamine}$, $R^2 = 0.999$). A limit of detection (LOD) was calculated by using formula 3σ/slope, where σ is the standard deviation of three blank solutions. The sensor A and sensor C thus exhibited a LOD of 38 nM (~0.005 mg/kg) and 0.24 μM (~0.03 mg/kg), respectively. Both values are much lower

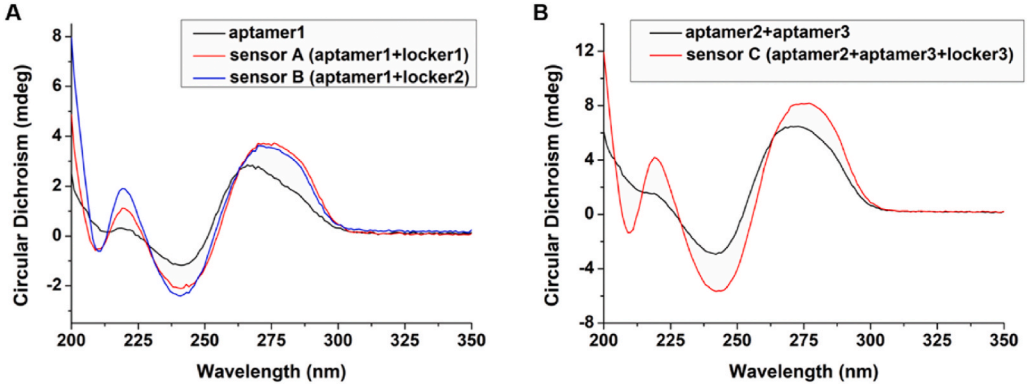

Fig. 2. (A) The CD spectra of apatmer1, sensor A (aptamer1+locker1), and sensor B (aptamer1+locker2); (B) The CD spectra of apatmer2+aptamer3, and sensor C (apatmer2+aptamer3+locker3).

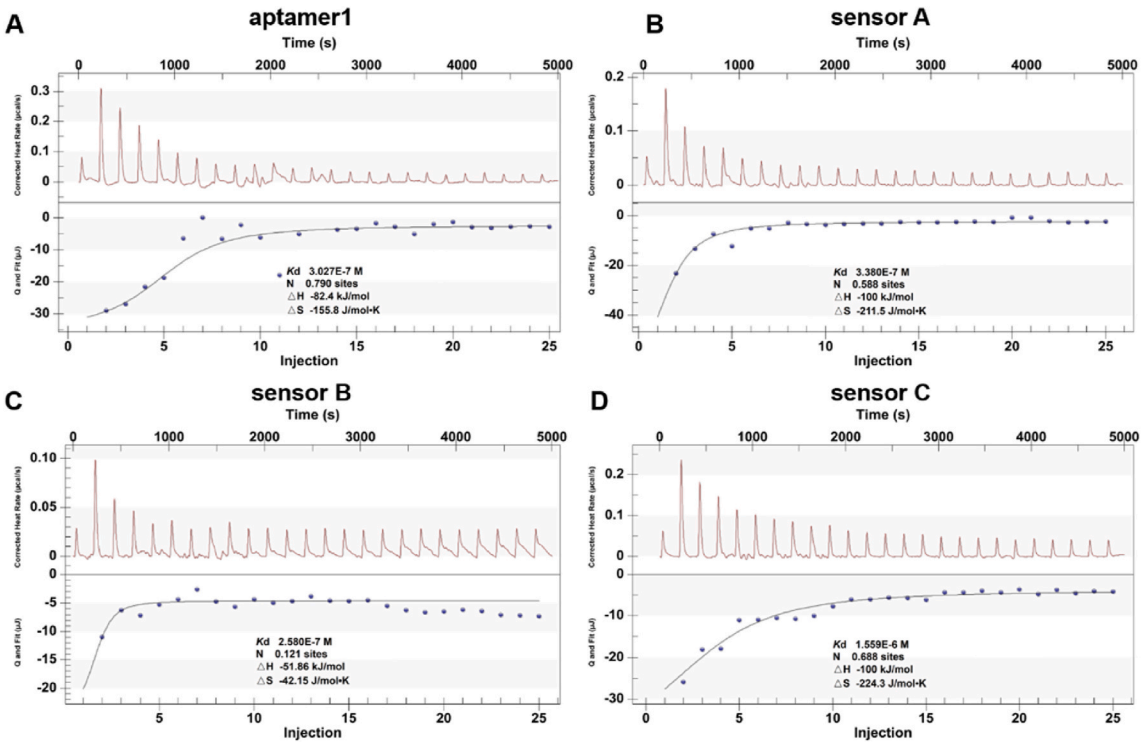

Fig. 3. Binding affinity characterization of the aptamer1 and DNA biosensors through using ITC. The DNA samples including (A) aptamer1, (B) "aptamer1-locker1" DNA complex, (C) "aptamer1-locker2" DNA complex and (D) "aptamer2-aptamer3-locker3" DNA complex were titrated with melamine.

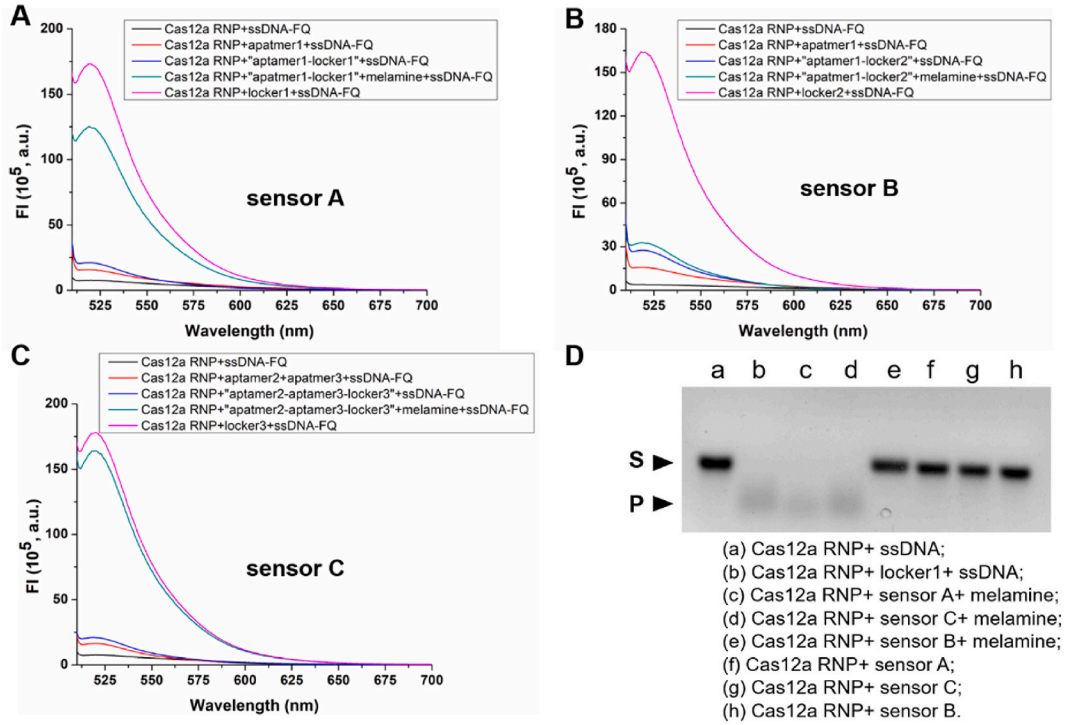

Fig. 4. Results of the designed "aptamer-locker" DNA sensors for melamine detection. (A) The fluorescence spectra of sensor A; (B) The fluorescence spectra of sensor B; (C) The fluorescence spectra of sensor C; (D) The PAGE analysis of the feasibility of sensors. A 50 nt ssDNA without secondary structure was used as the substrate (S), and the products (P) were visualized. Note: 200 μM melamine were added in each measurement.

than the safety level recommended by regulatory departments (1 mg/kg), demonstrating that these two biosensors can be used for high-efficiency melamine analysis. Compared to sensor A, the sensor C has a wider linear curve range. Therefore, it has advantages for detection of the samples containing high concentrated melamine. On the contrary, the sensor A would be chosen for determination of the trace melamine in products.

Moreover, the proposed method showed excellent selectivity over

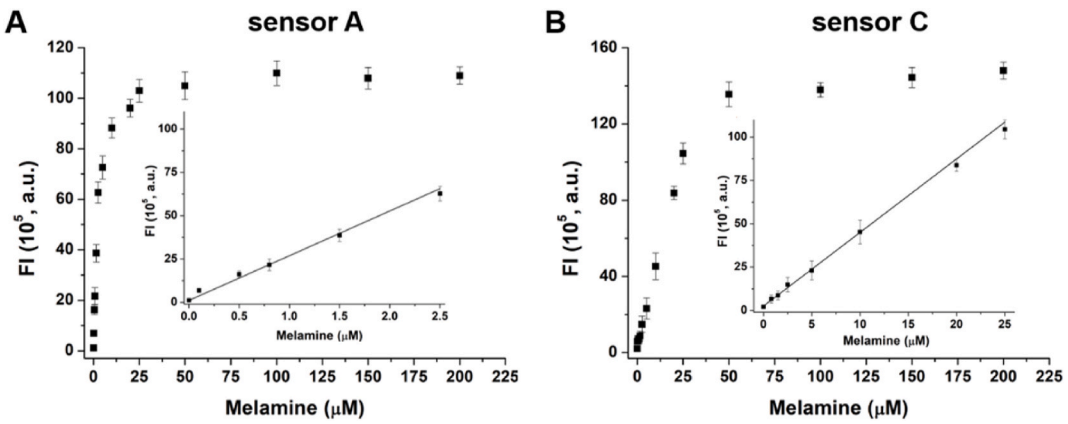

Fig. 5. The fluorescence intensity at 520 nm of (A) sensor A and (B) sensor C in the presence of different concentrations of melamine. Insets show the linear relationship between fluorescence and the melamine concentrations. Error bars represent the standard deviation of three repetitive experiments. The data were recorded by a fluorescence spectrophotometer F4600.

three melamine analogues, including cyanuric acid, ammeline and ammelide. As shown in Fig. S5, no detectable signal can be observed for 200 μM cyanuric acid, ammeline or ammelide.

3.4. Detection of melamine in milk

The feasibility of our method was demonstrated through detection of melamine in raw milk samples. Initially, three known concentrations of melamine (0.5 μM, 5 μM and 20 μM) were spiked with the whole milk samples that were pretreated by conventional methods (Gu et al., 2016; Jigyasa and Rajput 2018). As shown in Table 1, the recovery was acquired from 98% to 101.6% with an RSD (n = 3) between 1.72% and 2.63%, demonstrating the promise for practical use for monitoring melamine in milk. This performance is comparable with the results (Fig. S6) obtained using a traditional HPLC method (Ehling et al., 2007).

Taking advantage of the Cas12a RNP's collateral activity, researchers created a method termed DETECTER which achieved attomolar sensitivity for DNA detection (Chen et al., 2018). In addition, many other Cas12a-based fluorescent methods also showed ultra-high sensitivity (Broughton et al., 2020; Li et al. 2020a, 2020b; Wang et al., 2020). Hence, we assumed that our method might be able to measure melamine in milk without pretreatment. The proof-of-concept experiments were carried out by using the diluted milk. The locker1 DNA, ssDNA-FQ and Cas12a RNP were added, and the fluorescence signals were recorded. The results reveal that at least a tenfold dilution is required to get good analytical performance. Once again, we measured the recovery efficiencies of melamine in unpretreated milk (Table 1), which showed that both strategies get the similar results. In Table S2, the proposed method is compared with the currently-used melamine detection approaches. Accordingly, most methods require additional sample pretreatment steps, and thus take more time than ours. Herein, a standard assay for melamine testing can be completed within 20 min at 25 °C.

3.5. On-site analysis of melamine in milk

On-site test is critical for analyzing the toxic substances in dairy products. Previously, a personal glucose meter has been harnessed for melamine detection at home (Gu et al., 2015), achieving a LOD of 0.53 μM in 80% whole milk. In addition, a distance-based sensor (Li et al., 2018) was developed for the quantification of melamine in dairy products based on chip electrophoretic titration (ET) of moving neutralization boundary (NB) and EDTA photo-catalysis, achieving a LOD of 0.2 μM in 80% whole milk. As mentioned above, our method has an LOD down to 38 nM. Using a protable fluorimeter, we finnally conducted the on-site analysis of melamine in milk. Following the workflow illustrated in Fig. 1B, the fluorescence intensity at 520 nm was recorded and the linear curve (Fig. S7) was fit. Consequently, a good recovery efficiency of 98.2% was observed by measuring the unpretreated milk that was spiked with 5 μM melamine.

4. Conclusions

In summary, we herein develop a CRISPR/Cas12a-guided biosensing method for sensitive and rapid melamine analysis. Three strategies were adopted for designing the "aptamer-locker" DNA sensors. Coupling with a Cas12a-based fluorescent method, two sensors were found to be effective for quantitatively detecting the melamine in solution, achieving a limit of detection (LOD) as low as 38 nM. In addition, the proposed method showed high selectivity for melamine against its structural analogues. Good recovery efficiencies were obtained for the detection of melamine in pretreated milk. More importantly, our method can analyze melamine in milk without any pretreatment. A standard assay only requires less than 20 min under ambient temperatures. At last, the on-site test of melamine was achieved using a portable fluorimeter. By replacing the aptamers, the method demonstrated here can expand to develop biosensors for non-nucleic-acid targets.

Table 1
Application of the method for melamine analysis in real milk samples with or without pretreatment.

Milk samples	Spiked (μM)	Measured (μM)	Recovery (%)	RSD (n = 3, %)
1 (pretreated)	0.5	0.49	98.0	1.72
2 (pretreated)	5	5.08	101.6	2.21
3 (pretreated)	20	19.61	98.05	2.63
1 (unpretreated)	0.5	0.46	92.0	3.35
2 (unpretreated)	5	5.02	100.4	2.45
3 (unpretreated)	20	20.22	101.1	1.98

CRediT authorship contribution statement

Bin Qiao: Methodology, Data curation, Validation. **Jiakun Xu:** Resources, Data curation, Validation. **Wenhao Yin:** Investigation, Data curation, Validation. **Wanmeng Xin:** Investigation, Data curation, Validation. **Lixin Ma:** Resources. **Jie Qiao:** Conceptualization, Validation. **Yi Liu:** Conceptualization, Validation, Writing – review & editing, Supervision.

Declaration of competing interest

The authors declare that they have no known competing financial interests or personal relationships that could have appeared to influence the work reported in this paper.

Acknowledgements

This work was supported by the National Natural Science Foundation of China (NO. 21907027; 22007030), Project funded by China Postdoctoral Science Foundation (NO. 2019M662573) and Project funded by Natural Science Foundation of Hubei Province (NO. 2020CFB253).

Appendix A. Supplementary data

Supplementary data to this article can be found online at https://doi.org/10.1016/j.bios.2021.113233.

References

Alipour, M., Jalili, S., Shirzad, H., Dezfouli, E.H., Fouani, M.H., Sadeghan, A.A., Bardania, H., Hosseinkhani, S., 2020. Mikrochim. Acta 87, 628–640.
Broughton, J.P., Deng, X., Yu, G., Fasching, C.L., Servellita, V., Singh, J., Miao, X., Streithorst, J.A., Granados, A., Sotomayor-Gonzalez, A., Zorn, K., Gopez, A., Hsu, E., Gu, W., Miller, S., Pan, C.Y., Guevara, H., Wadford, D.A., Chen, J.S., Chiu, C.Y., 2020. Nat. Biotechnol. 38, 870–874.
Chen, D., Zhao, Y., Miao, H., Wu, Y., 2015. Talanta 134, 144–152.
Chen, J.S., Ma, E., Harrington, L.B., Da Costa, M., Tian, X., Palefsky, J.M., Doudna, J.A., 2018. Science 360, 436–439.
Choi, J.W., Min, K.M., Hengoju, S., Kim, G.J., Chang, S.I., deMello, A.J., Choo, J., Kim, H. Y., 2016. Biosens. Bioelectron. 80, 182–186.
Domingo Edo, C., Tireli, A.A., Nunes, C.A., Batista, A.V., Guerreiro, M.C., Pinto, S.M., 2015. Talanta 132, 535–540.
Du, Y.C., Wang, S.Y., Wang, Y.X., Ma, J.Y., Wang, D.X., Tang, A.N., Kong, D.M., 2021. Biosens. Bioelectron. 171, 112734–112740.
Duan, X., Dai, X.X., Wang, T., Liu, H.L., Sun, S.C., 2015. Hum. Reprod. 30, 1643–1652.
Ehling, S., Tefera, S., Ho, I.P., 2007. Food Addit. Contam. A. 24, 1319–1325.
Fozouni, P., Son, S., Díaz de León Derby, M., Knott, G.J., Gray, C.N., D'Ambrosio, M.V., Zhao, C., Switz, N.A., Kumar, G.R., Stephens, S.I., Boehm, D., Tsou, C.L., Shu, J., Bhuiya, A., Armstrong, M., Harris, A.R., Chen, P.Y., Osterloh, J.M., Meyer-Franke, A., Joehnk, B., Walcott, K., Sil, A., Langelier, C., Pollard, K.S., Crawford, E. D., Puschnik, A.S., Phelps, M., Kistler, A., DeRisi, J.L., Doudna, J.A., Fletcher, D.A., Ott, M., 2020. Cell 184, 323–333.
Fu, C.L., Liu, C., Li, Y., Guo, Y.J., Luo, F., Wang, P.L., Guo, L.H., Qiu, B., Lin, Z.Y., 2016. Anal. Chem. 88, 10176–10182.
Gootenberg, J.S., Abudayyeh, O.O., Kellner, M.J., Joung, J., Collins, J.J., Zhang, F., 2018. Science 360, 439–444.
Gootenberg, J.S., Abudayyeh, O.O., Lee, J.W., Essletzbichler, P., Dy, A.J., Joung, J., Verdine, V., Donghia, N., Daringer, N.M., Freije, C.A., Myhrvold, C., Bhattacharyya, R.P., Livny, J., Regev, A., Koonin, E.V., Hung, D.T., Sabeti, P.C., Collins, J.J., Zhang, F., 2017. Science 356, 438–442.
Gu, C., Lan, T., Shi, H., Lu, Y., 2015. Anal. Chem. 87, 7676–7682.
Gu, C., Xiang, Y., Guo, H., Shi, H., 2016. Analyst 141, 4511–4517.
Guan, N., Fan, Q., Ding, J., Zhao, Y., Lu, J., Ai, Y., Xu, G., Zhu, S., Yao, C., Jiang, L., Miao, J., Zhang, H., Zhao, D., Liu, X., Yao, Y., 2009. NEW. ENGL. J. MED. 360, 1067–1074.
Hu, X., Chang, K., Wang, S., Sun, X., Hu, J., Jiang, M., 2018. PloS One 13, e0201626.
Jigyasa, Rajput, J.K., 2018. Biosens. Bioelectron. 120, 153–159.
Lei, H., Shen, Y., Song, L., Yang, J., Chevallier, O.P., Haughey, S.A., Wang, H., Sun, Y., Elliott, C.T., 2010. Aanl. Chim. Acta. 665, 84–90.
Li, B., Xia, A., Zhang, S., Suo, T., Ma, Y., Huang, H., Zhang, X., Chen, Y., Zhou, X., 2020a. Biosens. Bioelectron. 173, 112619.
Li, C.Y., Zheng, B., Liu, Y.H., Gao, J.L., Zheng, M.Q., Pang, D.W., Tang, H.W., 2020b. Biosens. Bioelectron. 169, 112650.
Myhrvold, C., Freije, C.A., Gootenberg, J.S., Abudayyeh, O.O., Metsky, H.C., Durbin, A. F., Kellner, M.J., Tan, A.L., Paul, L.M., Parham, L.A., Garcia, K.F., Barnes, K.G., Chak, B., Mondini, A., Nogueira, M.L., Isern, S., Michael, S.F., Lorenzana, I., Yozwiak, N.L., MacInnis, B.L., Bosch, I., Gehrke, L., Zhang, F., Sabeti, P.C., 2018. Science 360, 444–448.
Nascimento, C.F., Santos, P.M., Pereira-Filho, E.R., Rocha, F.R.P., 2017. Food Chem. 221, 1232–1244.
Qiao, J., Li, W., Lin, S., Sun, W., Ma, L., Liu, Y., 2019. Commun. Biol. 2, 161–166.
Qiao, J., Lin, S., Sun, W., Ma, L., Liu, Y., 2020. Chem. Commun. 56, 12616–12619.
Wang, D.X., Wang, J., Du, Y.C., Ma, J.Y., Wang, S.Y., Tang, A.N., Kong, D.M., 2020. Biosens. Bioelectron. 168, 112556.
Wang, R., Qian, C., Pang, Y., Li, M., Yang, Y., Ma, H., Zhao, M., Qian, F., Yu, H., Liu, Z., Ni, T., Zheng, Y., Wang, Y., 2021. Biosens. Bioelectron. 172, 112766–112773.
Wang, T.T., Xuan, R.R., Ma, J.F., Tan, Y., Jin, Z.F., Chen, Y.H., Zhang, L.H., Zhang, Y.K., 2016. Anal. Bioanal. Chem. 408, 6671–6677.
Xie, Z., Lei, J., Yang, M., Li, Y., Geng, X., Liu, S., Wang, J., 2019. Biosens. Bioelectron. 127, 200–206.
Xiong, Y., Zhang, J., Yang, Z., Mou, Q., Ma, Y., Xiong, Y., Lu, Y., 2020. J. Am. Chem. Soc. 142, 207–213.
Yu, H.Q., Miyoshi, D., Sugimoto, N., 2006. J. Am. Chem. Soc. 128, 15461–15468.